

Research Article

Integration of UV-cured Ionogel Electrolyte with Carbon Paper Electrodes

Stephanie Flores Zopf and Matthew J. Panzer *

Department of Chemical & Biological Engineering, Tufts University, Medford, MA 02155, USA

* **Correspondence:** E-mail: matthew.panzer@tufts.edu; Tel: +1 (617) 627-4633; Fax: +1 (617) 627-3991.

Abstract: A test bed with a coplanar architecture is employed to investigate the integration of an *in situ* cross-linked, polymer-supported ionogel with several commercially available, high surface area carbon paper electrodes. Specifically, a UV-cured poly(ethylene glycol) diacrylate (PEGDA)-supported ionogel electrolyte film is formed *in situ* against a variety of porous electrodes comprising: a carbon fiber paper, a carbon aerogel paper, and four carbon nanotube-based papers. Electrochemical impedance spectroscopy measurements reveal that the relative performance of a particular carbon paper with the neat ionic liquid is not necessarily indicative of its behavior when integrated with the solid ionogel electrolyte. The coplanar test bed can therefore serve as a useful tool to help guide the selection of suitable carbon-based electrode structures for supercapacitors that incorporate UV-cured ionogels created *in situ* for wearable energy storage applications.

Keywords: supercapacitor; ionogel; ionic liquid; carbon paper; energy storage

1. Introduction

An increasing reliance on portable electronics has motivated the recent investigation of wearable energy storage systems. Viable energy storage solutions for wearable applications should be safe for the consumer, lightweight, physically flexible, and straightforward to manufacture. Use of a solid-state gel electrolyte may enable a fully printable device architecture that can satisfy all of these requirements [1]. Ionic liquid-based gels, or ionogels, offer an attractive way to realize a safe supercapacitor electrolyte due to the negligible vapor pressure of the ionic liquid, which renders it nonvolatile and nonflammable.

Ionogels are composite materials that consist of an ionic liquid and a solid support matrix of organic, inorganic, or hybrid composition. The matrix can be formed by physical coagulation of a solid additive (*e.g.* carbon nanotubes, fumed silica, organic gelators), or through chemical

reaction [2]. Electrolyte gels that employ a polymer-based matrix have widely been used to demonstrate flexible supercapacitor prototypes due to their physical integrity [3,4]. It has recently been shown that ionogels formed *in situ* by UV-initiated free radical polymerization are extremely simple to fabricate, and possess desirable characteristics as solid electrolytes [5,6]. However, few studies have explored the integration of UV-cured ionogel electrolytes with carbon electrodes due to the inherent difficulty of irradiating a thin film of gel precursor solution sandwiched between opaque carbon electrodes with UV light [7].

Solid-state, flexible supercapacitor prototype assembly can be broadly classified into two categories: (1) a multi-step approach, whereby the surfaces of two distinct carbon electrodes are first coated with a gel electrolyte and subsequently sandwiched together [8–12], or (2) a one-step approach, whereby a gel electrolyte is formed *in situ* against two carbon electrodes that have already been arranged in their desired final geometry within the device [13,14]. Although the multi-step process is feasible in a laboratory setting, a one-step process would provide a simpler approach to both scale-up and large-scale production. Furthermore, by eliminating the need to mechanically press two halves of the device together, one-step assembly greatly reduces the possibility of damaging the typically fragile high surface area carbon electrodes employed in supercapacitors. With several groups currently developing novel types of high surface area carbon-based electrodes [15–19], there is a critical need to understand how ionogel electrolytes can be effectively combined with these structures *in situ*.

The work described here examines the integration of an *in situ* UV-cured poly(ethylene glycol) diacrylate (PEGDA)-supported ionogel electrolyte [6] with several commercially available, high surface area carbon paper electrodes. In order to cure the gel electrolyte *in situ* adjacent to both carbon electrodes, a coplanar test bed architecture was employed. This approach served as a repeatable means of forming a thin UV-cured ionogel film in contact with different pairs of opaque carbon electrodes in a single step. In addition, a direct comparison of the electrical response of the ionogel electrolyte with that of the neat ionic liquid, 1-ethyl-3-methylimidazolium bis(trifluoromethylsulfonyl)imide (EMI TFSI), was performed in order to examine the hypothesis that the performance of a particular carbon electrode with neat EMI TFSI is directly correlated to its performance with the PEGDA-supported ionogel electrolyte.

2. Materials and Method

2.1. Coplanar Test Bed Assembly

Ionogel-carbon paper electrode assemblies were fabricated with a coplanar electrode geometry on glass microscope slides. PTFE pipe thread tape was used to define a rectangular area of 60 mm² (12 mm × 5 mm), inside which the active components of the device were located. A portion of each carbon paper was initially immersed in melted paraffin wax (McMaster Carr). After this treatment, the carbon paper was cut such that an uncoated carbon paper projected area of 25 mm² (5 mm × 5 mm) was exposed directly adjacent to the edge of the paper treated by the paraffin wax. This area represents the active part of each electrode that was wetted by electrolyte. Two electrodes were cut out in this fashion and placed flat on the glass slide within the area bordered by the PTFE tape. A gap of 2 mm was maintained between the edges of the carbon paper electrodes for all assemblies. An electrolyte solution volume of 30 μL (either neat ionic liquid or the ionogel precursor

solution, see below) was pipetted into the PTFE-bounded region containing the carbon electrodes from above. Electrical contact was made using nickel-plated steel micro-alligator clips that gripped the paraffin-treated portion of the carbon papers against the glass slide. Ionogel devices were assembled and tested in a nitrogen-filled glovebox (< 1 ppm oxygen and water vapor). Devices made with the neat ionic liquid were assembled and tested under ambient laboratory conditions.

2.2. High Surface Area Carbon Papers and the Ionogel Electrolyte

High surface area carbon papers were procured from three sources. Graphitized carbon fiber paper (CFP), manufactured by Engineered Fibers Technology, was obtained from an online materials supplier. Carbon aerogel paper (CAGP) was manufactured by and obtained from Marketech International. Carbon nanotube paper (CNTP) was manufactured by and obtained from Inorganic Specialists, Inc.; four different variations of this paper were examined (CNTP1, CNTP2, CNTP3, and CNTP4). The sheet resistances of all carbon papers were measured using a four-point probe instrument (Creative Design Engineering). The manufacturer-reported specific surface areas and the measured sheet resistance values of each carbon paper are summarized in Table 1.

Table 1. Properties of high surface area carbon paper electrodes.

Carbon Electrode	Reported Specific Surface Area (m ² g ⁻¹)	Measured Sheet Resistance (Ohm sq. ⁻¹)	Binder Present?
CFP	80	0.5	yes
CAGP	600	1.3	no
CNTP1	60	5.1	no
CNTP2	180	5.0	no
CNTP3	220	14.7	no
CNTP4	400	3.4	no

The solid ionogel electrolyte was fabricated following the method of Visentin and Panzer [6]. The ionic liquid, 1-ethyl-3-methylimidazolium bis(trifluoromethylsulfonyl)imide (EMI TFSI), was obtained from EMD Chemicals. The polymer scaffold precursor, polyethylene glycol diacrylate (PEGDA), and UV-initiator, 2-hydroxy-2-methylpropiophenone, were obtained from Sigma Aldrich. A polymer content of 16% wt. PEGDA was selected based on its ease of handling and flexible character [6]. After dispensing the ionogel precursor solution on top of the coplanar electrode assembly, UV irradiation for 3 min (from the top) was used to create the gel electrolyte. All chemicals used to create the ionogel electrolyte were stored and used in the nitrogen-filled glovebox.

Cyclic voltammetry (CV) and electrical impedance spectroscopy (EIS) were performed using a potentiostat with a built-in frequency response analyzer (VersaSTAT 3, Princeton Applied Research). CV was conducted at a voltage sweep rate of 1 mV s⁻¹ within a window of -1.5 V to +1.5 V (vs. open circuit); at least three cycles were recorded to ensure repeatability between successive voltage sweeps. For each EIS measurement, the frequency was logarithmically swept from 10 kHz to 1 mHz. The RMS amplitude of the AC signal employed was 10 mV (DC offset of 0 V vs. open circuit).

3. Results and Discussion

3.1. Carbon Paper Electrodes

Scanning electron microscopy (SEM) was used to examine the microstructure of the various carbon papers employed in this study. Figure 1 shows representative SEM images obtained for the carbon fiber paper (CFP), carbon aerogel paper (CAGP), and carbon nanotube paper #3 (CNTP3); it should be noted that the four CNTP papers (CNTP1-4) all appeared visually similar when viewed under 5000 \times magnification.

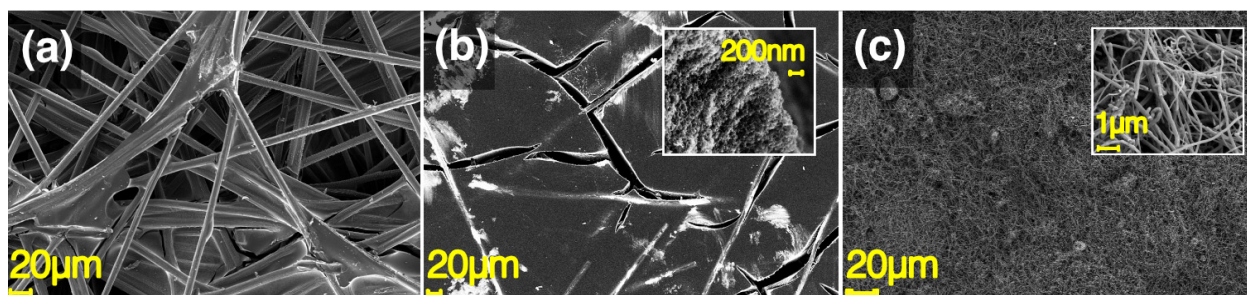


Figure 1. SEM images of the three main carbon paper types employed: (a) carbon fiber paper (CFP); (b) carbon aerogel paper (CAGP); (c) carbon nanotube paper #3 (CNTP3), which is representative of all four CNTP materials used in this study. Insets to (b) and (c) show the pore structures of these papers at higher magnification.

CFP is a porous carbon paper that is typically used for laboratory scale fuel cell development. It consists of a graphitized network of resin-bonded carbon fibers, and, as seen in Figure 1a, CFP exhibits the largest apparent pore size among all of the papers utilized in this study. It is important to note that the CFP material was the only electrode studied that contained a binder for physical support (Figure 1a).

According to its manufacturer (Marketch International, Inc.), the CAGP material is prepared by a sol-gel method from a resorcinol-formaldehyde precursor, which, post-reaction, is carbonized to create a carbon foam with high porosity and surface area. To create a robust paper electrode, the CAGP also contains carbon fibers for mechanical support (Figure 1b). Inside the micron-scale cracks present on the surface of the CAGP electrodes, the nanoporous carbon foam structure is visible (pore size of approximately 80 nm, see inset to Figure 1b), which gives the CAGP material its very high reported specific surface area of 600 m² g⁻¹.

Four types of carbon nanotube paper were obtained from Inorganic Specialists, Inc. (CNTP1-4). All of the CNTP materials consist of 100% carbon nanotubes/fibers, with no binder present (Figure 1c). Such papers are fabricated by dispersing carbon nanotubes/fibers in water, then filtering the suspension through a porous support membrane to produce a carbon filter cake [20]. Due to the absence of any binder material, the CNTP electrodes were the most fragile to handle. Variation in the reported specific surface areas of the four CNTP materials utilized in this study was likely achieved by the manufacturer incorporating carbon nanotubes of different diameters and/or lengths, as evidenced by SEM imaging at high magnification (inset to Figure 1c).

3.2. Cyclic voltammetry

Figure 2 displays the CV curves obtained for coplanar test beds fabricated with the six different types of carbon paper electrodes examined and the ionogel electrolyte; current values are normalized by the total mass of two electrodes. Each curve exhibits an approximately rectangular shape, indicating that capacitive behavior was observed for all of the carbon papers. If it is assumed to be independent of voltage, the capacitance of each device can be calculated directly from the current values measured during the CV sweeps via:

$$C = \frac{I}{\left(\frac{dV}{dt}\right)}$$

The positive current value measured at 0 V on the CV graph was used to calculate the capacitance of each device (the absolute values of the negative currents were nearly identical to the positive current values). Gravimetric capacitances for each electrode type integrated with the ionogel electrolyte are summarized in Table 2. The capacitance values can be approximately correlated with the reported surface areas of the carbon papers (shown in Table 1), with one notable exception; namely, the capacitance of the CFP device (0.02 F g^{-1}) was nearly two orders of magnitude lower than was observed for the other electrode papers. Although its reported specific surface area was relatively low ($80 \text{ m}^2 \text{ g}^{-1}$), the CFP material exhibited significantly lower capacitance compared to the CNTP1 material, which claimed a similar specific surface area of $60 \text{ m}^2 \text{ g}^{-1}$. This discrepancy is likely due to the presence of the binder in CFP (Figure 1a), which reduces either the wettability of the electrode by the ionogel precursor solution, and/or the effective (conductive) electrode surface area.

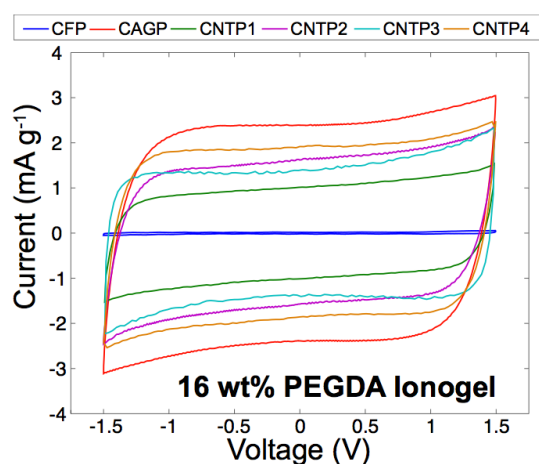


Figure 2. Cyclic voltammograms of test beds containing different carbon paper electrodes with 16 wt% PEGDA ionogel electrolyte (third cycle shown in each case). A scan rate of 1 mV s^{-1} was used.

3.3. Electrical Impedance Spectroscopy

Figure 3 displays Bode plots of the phase angle of impedance (ϕ) obtained for each carbon

paper type, together with the neat EMI TFSI ionic liquid (Figure 3a) or the ionogel electrolyte (Figure 3b). The frequency at which the phase angle reaches -45° (f_0) is termed the “switching frequency,” where a device transitions from exhibiting primarily resistive to primarily capacitive behavior. Comparison of the neat EMI TFSI and ionogel electrolytes shown in Figure 3 reveals that the neat EMI TFSI devices uniformly exhibited switching frequencies approximately five times faster than their ionogel counterparts. This difference is due to the presence of the cross-linked PEGDA scaffold in the ionogel, which impedes the polarization response of the ions [6]. The switching frequency for CFP with the ionogel electrolyte ($f_0 = 6.3$ Hz) was observed to be approximately three orders of magnitude larger than for the other carbon papers examined (f_0 varies between 2–10 mHz), as seen in Figure 3b. It should be pointed out that these values are lower than those typically reported for supercapacitor prototypes, due to the coplanar electrode architecture employed here. However, a comparison of the EIS behavior of the various carbon paper electrodes for a given electrolyte (either neat ionic liquid or the ionogel) can illuminate differences in the relative performance of each carbon structure. The comparatively fast switching frequency observed for CFP with both electrolyte types is attributed to the large, open pore structure defined by the carbon fibers of this material (Figure 1a), which facilitates ready access to the EMI and TFSI ions for rapid double layer formation and rearrangement. However, the low effective surface area of the CFP material that enables a fast polarization response also leads to the lowest observed capacitance (Figure 2).

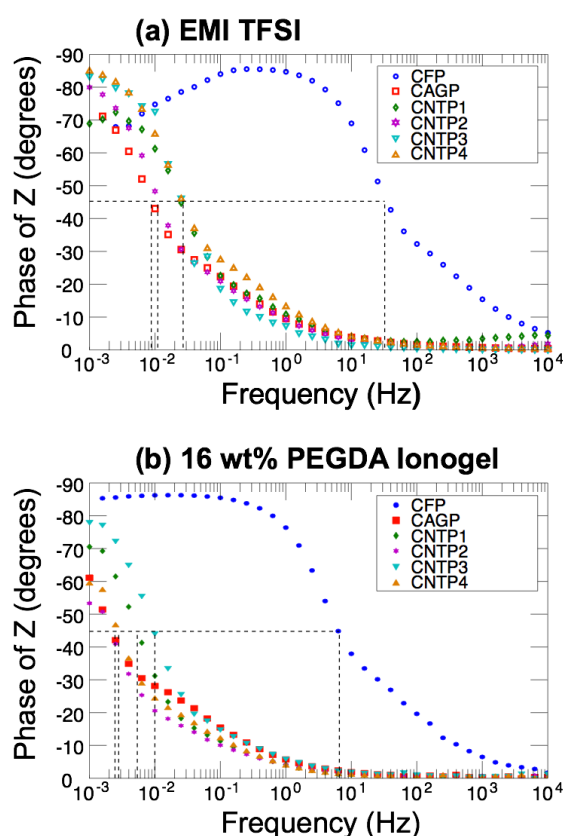


Figure 3. Bode plots of the phase angle of impedance for test beds containing: (a) neat EMI TFSI electrolyte; (b) 16 wt% PEGDA ionogel electrolyte.

The magnitude of impedance ($|Z|$) versus frequency data measured using the neat ionic liquid and ionogel electrolyte test beds are shown in Figure 4. While it is noted that the equivalent series resistance (ESR) values obtained here are much larger than those of typical supercapacitor devices (due to the coplanar structure of the test bed), relative comparisons among the carbon papers are highly informative. The CAGP and CFP materials exhibited lower ESR values (taken to be equal to $|Z|$ at $f = 10$ kHz) compared to the other electrode materials with both neat EMI TFSI (Figure 4a) as well as with the ionogel electrolyte (Figure 4b), as summarized in Table 2. This result was expected since these two electrode materials possessed the lowest measured sheet resistances (Table 1). However, a different trend is observed within the group of CNTP materials upon comparing their behavior with the neat ionic liquid versus the ionogel electrolyte. The order of carbon nanotube paper sheet resistances, from highest to lowest, is: CNTP3 > CNTP1 \approx CNTP2 > CNTP4 (Table 1). This trend is mirrored in the ordering of device ESR values when EMI TFSI is used as an electrolyte (Figure 4a), but is not the case when the ionogel electrolyte is employed (Figure 4b). As seen in Table 2, the ESR value of the CNTP3 device with the ionogel electrolyte (9.74 k Ω) is, in fact, lower than those for both the CNTP1 and CNPT2 devices (11.7 k Ω and 10.2 k Ω respectively). Furthermore, CNTP4, which exhibited the lowest measured sheet resistance among the four carbon nanotube-based papers and demonstrated a low ESR value when paired with the neat ionic liquid (0.615 k Ω), displayed an unexpectedly large relative increase in ESR when integrated with the solid ionogel electrolyte (6.98 k Ω). As shown in Table 2, the relative increase in ESR between the ionogel and the neat EMI TFSI responses ranged from 3.9 \times (for CNTP3) to as large as 11.3 \times (for CNTP4).

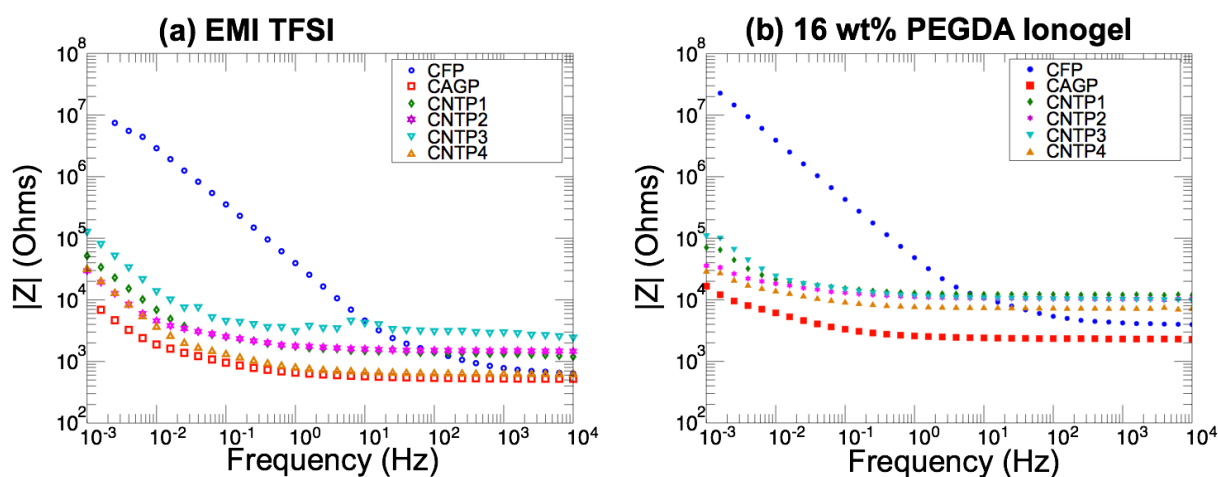


Figure 4. Magnitude of impedance, $|Z|$, for test beds containing: (a) neat EMI TFSI electrolyte; (b) 16 wt% PEGDA ionogel electrolyte.

Table 2. Performance of test bed devices with 16 wt% PEGDA ionogel.

Carbon Electrode	Specific Capacitance (F g _{electrodes} ⁻¹)	Equiv. Series Resistance (kΩ)	ESR_{ionogel}/ESR_{EMI TFSI} (-)
CFP	0.02	3.88	6.1
CAGP	2.33	2.25	4.3
CNTP1	0.97	11.7	9.8
CNTP2	1.63	10.2	7.0
CNTP3	1.30	9.74	3.9
CNTP4	1.87	6.98	11.3

Since identical electrolyte solutions and fabrication conditions were employed for each carbon paper electrode test bed, one may attribute differences in performance of the various electrode materials when changing from the ionic liquid to the ionogel electrolyte to differences in wettability and/or interfacial compatibility. More specifically, the formation of the cross-linked PEGDA scaffold inside the ionic liquid during UV-curing of the ionogel precursor solution may lead to adsorption of the polymer on the carbon electrode surface, causing an increased carbon/electrolyte interfacial resistance. This possibility is expected to depend strongly on the detailed nature of the pore structure and surface chemical functionalization of each carbon paper, and is worthy of further investigation. Alternatively, differing degrees of pore mouth blockage among the various carbon papers by the cross-linked PEGDA scaffold may also lead to unexpected relative changes in ESR when switching from the neat ionic liquid to an ionogel electrolyte. Given that the two-electrode double layer capacitance of both the neat EMI TFSI as well as the ionogel electrolyte is approximately 5 μF cm⁻² for planar electrodes [6], it is clear that the ionogel precursor solution did not fully penetrate the porous structure of any of these carbon papers during the test bed fabrication procedure (as demonstrated by the low gravimetric capacitance values measured by CV, Table 2). In addition, the high ESR values observed for these devices may also have limited the gravimetric capacitance values achieved. A modified test bed fabrication protocol wherein the ionogel precursor solution is actively drawn into the porous carbon papers (*i.e.* by vacuum filling) is currently being developed in order to increase the gravimetric capacitance values and to clarify the issue of seeming unpredictable relative ESR changes when transitioning from an ionic liquid to an ionogel electrolyte.

4. Conclusion

In order to begin integrating UV-cured solid ionogel electrolytes, a promising class of emergent materials for supercapacitors, with high surface area carbon paper electrodes *in situ*, an understanding of the relative compatibility of the ionogel with different carbon electrode materials is required. The coplanar test bed geometry utilized here represents one schema by which this integration might be achieved, and it also provides a straightforward way to compare the electrical response of an ionogel electrolyte with its neat ionic liquid analog. Furthermore, initial results using this test bed have revealed anomalous trends in the relative increase of device equivalent series resistance observed for the use of a 16 wt% PEGDA ionogel compared to the neat ionic liquid that highlight the need to better understand the wetting and interfacial surface behavior at the electrode/electrolyte interface. These findings can help guide future efforts regarding the *in situ*

integration of ionogel electrolytes with porous carbon electrodes for wearable energy storage applications.

Acknowledgments

The authors wish to acknowledge Adam Visentin and Ariel Horowitz for useful discussions, Dr. Anna Oshero for collecting the SEM images, and Changqiong Zhu for measuring the carbon paper sheet resistances. SEM images and sheet resistance values were obtained at the Center for Nanoscale Systems (CNS), a member of the National Nanotechnology Infrastructure Network (NNIN), which is supported by the National Science Foundation under NSF award no. ECS-0335765. CNS is part of Harvard University. The authors gratefully acknowledge financial support from the Science, Mathematics and Research for Transformation scholarship, the US Army Natick Soldier Research, Development and Engineering Center, and the National Science Foundation (award no. ECCS-1201935).

Conflict of interest

All authors declare no conflicts of interest in this paper.

References

1. Kaempgen M, Chan CK, Ma J, et al. (2009) Printable thin film supercapacitors using single-walled carbon nanotubes. *Nano Lett* 9: 1872-1876.
2. Le Bideau J, Viau L, Vioux A. (2011) Ionogels, ionic liquid based hybrid materials. *Chem Soc Rev* 40: 907-925.
3. Sung J-H, Kim S-J, Lee K-H. (2004) Fabrication of all-solid-state electrochemical microcapacitors. *J Power Sources* 133: 312-319.
4. Sung J-H, Kim S-J, Jeong S-H, et al. (2006) Flexible micro-supercapacitors. *J Power Sources* 162: 1467-1470.
5. Stępniaak I, Andrzejewska E. (2009) Highly conductive ionic liquid based ternary polymer electrolytes obtained by in situ photopolymerisation. *Electrochim Acta* 54: 5660-5665.
6. Visentin AF, Panzer MJ. (2012) Poly(ethylene glycol) diacrylate-supported ionogels with consistent capacitive behavior and tunable elastic response. *ACS Appl Mater Interfaces* 4: 2836-2839.
7. Yang C-M, Ju JB, Lee JK, et al. (2005) Electrochemical performances of electric double layer capacitor with UV-cured gel polymer electrolyte based on poly[(ethylene glycol)diacrylate]-poly(vinylidene fluoride) blend. *Electrochim Acta* 50: 1813-1819.
8. Meng C, Liu C, Chen L, et al. (2010) Highly flexible and all-solid-state paperlike polymer supercapacitors. *Nano Lett* 10: 4025-4031.
9. Choi BG, Hong J, Hong WH, et al. (2011) Facilitated ion transport in all-solid-state flexible supercapacitors. *ACS Nano* 5: 7205-7213.
10. Hu S, Rajamani R, Yu X. (2012) Flexible solid-state paper based carbon nanotube supercapacitor. *Appl Phys Lett* 100: 104103.
11. Kang YJ, Chung H, Han C-H, et al. (2012) All-solid-state flexible supercapacitors based on

-
- papers coated with carbon nanotubes and ionic-liquid-based gel electrolytes. *Nanotechnology* 23: 065401.
12. Jung HY, Karimi MB, Hahm MG, et al. (2012) Transparent, flexible supercapacitors from nano-engineered carbon films. *Sci Rep* 2: 773.
 13. Pech D, Brunet M, Durou H, et al. (2010) Ultrahigh-power micrometre-sized supercapacitors based on onion-like carbon. *Nature Nanotech* 5: 651-654.
 14. El-Kady MF, Kaner RB. (2013) Scalable fabrication of high-power graphene micro-supercapacitors for flexible and on-chip energy storage. *Nature Commun* 4: 1475.
 15. Zhai Y, Dou Y, Zhao D, et al. (2011) Carbon materials for chemical capacitive energy storage. *Adv Mater* 23: 4828-4850.
 16. Liu C, Yu Z, Neff D, et al. (2010) Graphene-based supercapacitor with an ultrahigh energy density. *Nano Lett* 10: 4863-4868.
 17. Gallego AKC, Rincon ME. (2006) Carbon nanofiber and PEDOT-PSS bilayer systems as electrodes for symmetric and asymmetric electrochemical capacitor cells. *J Power Sources* 162: 743-747.
 18. Yang X, Zhu J, Qiu L, et al. (2011) Bioinspired effective prevention of restacking in multilayered graphene films: towards the next generation of high-performance supercapacitors. *Adv Mater* 23: 2833-2838.
 19. Hulicova-Jurcakova D, Seredych M, Lu GQ, et al. (2009) Combined effect of nitrogen- and oxygen-containing functional groups of microporous activated carbon on its electrochemical performance in supercapacitors. *Adv Funct Mater* 19: 438-447.
 20. Gou J, Tang Y, Liang F, et al. (2010) Carbon nanofiber paper for lightning strike protection of composite materials. *Composites: Part B* 41: 192-198.

© 2014, Matthew J. Panzer, licensee AIMS Press. This is an open access article distributed under the terms of the Creative Commons Attribution License (<http://creativecommons.org/licenses/by/4.0>)